Instituto Politécnico Nacional

Centro de Investigación en Ciencia Aplicada y Tecnología Avanzada
CICATA, Legaria 694. Col. Irrigación, C.P. 11500, México D.F., México
http://www.cicata.ipn.mx

"PHOTOTHERMAL DIGITAL LOCK-IN SHADOWGRAPH TECHNIQUE FOR MATERIALS THERMALCHARACTERIZATION."

by

ERNESTO MARÍN MOARES (Ph.D)
emarinm@ipn.mx   emarin63@yahoo.es (preferable)

The Abdus Salam
International Centre
for Theoretical Physics

Winter College on Optics: Advanced Optical Techniques for Bio-Imaging
February 13-24, 2017

OUTLINE:

1. THERMAL WAVE PHYSICS. PHOTOTHERMAL TECHNIQUES. THERMAL CHARACTERIZATION OF MATERIALS

2. THE PHOTOTHERMAL BEAM AND MULTIBEAM DEFLECTION TECHNIQUES

3. THE PHOTOTHERMAL SHADOWGRAPH METHOD

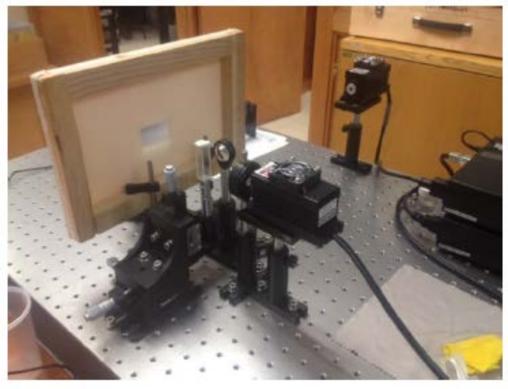

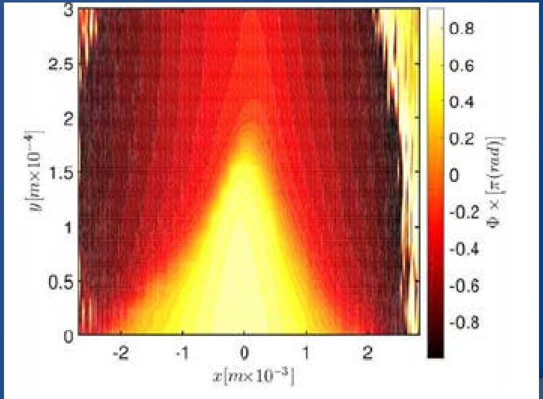

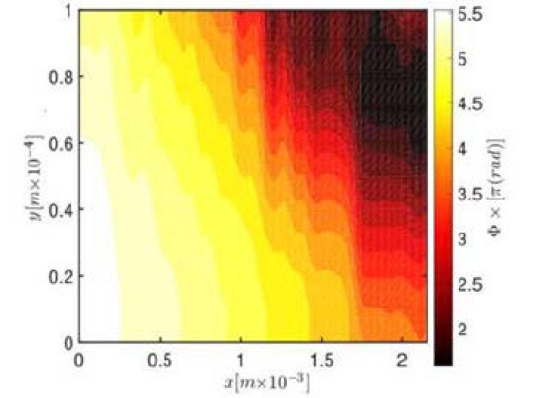

1st PART:
THERMAL WAVE PHYSICS
THE PHOTOTHERMAL TECHNIQUES
THERMAL CHARACTERIZATION OF MATERIALS

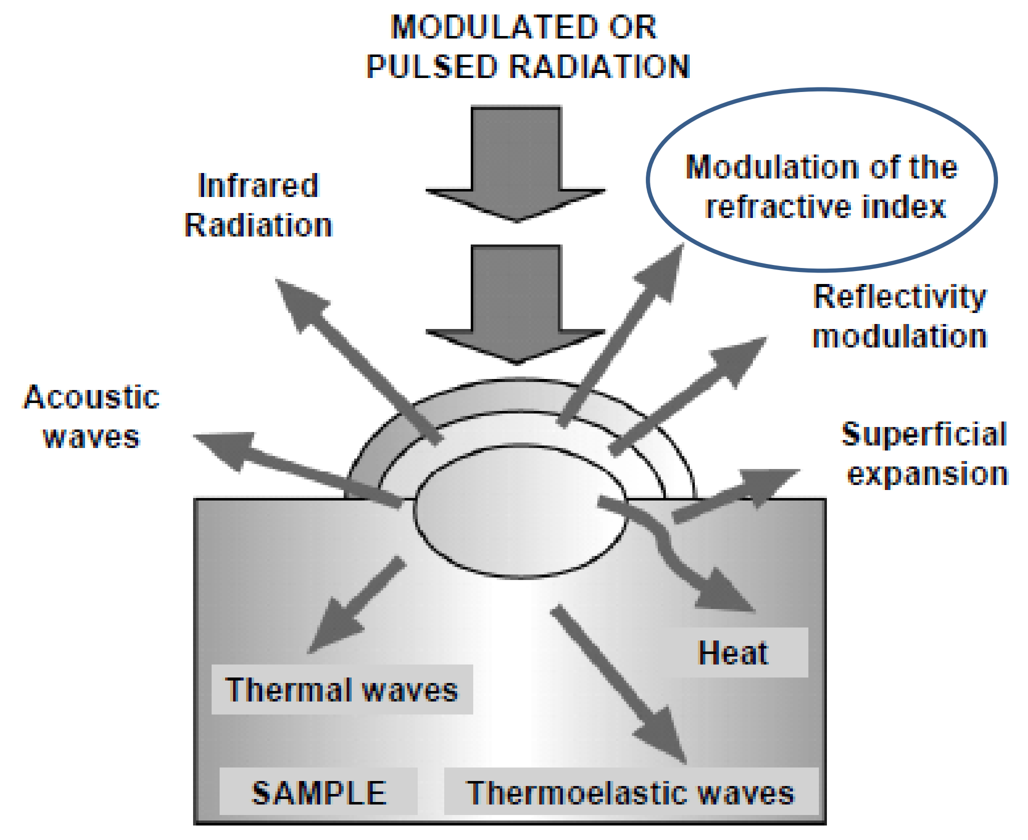

PRINCIPLES OF PHOTOTHERMAL TECHNIQUES

Intensity periodical modulated light beam

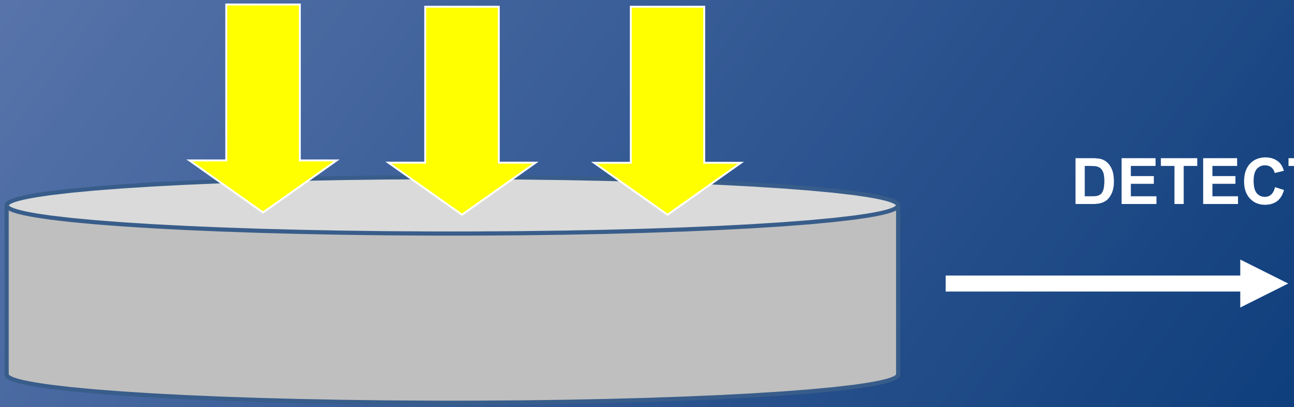

DETECTION SYSTEM

Mechanisms involved in the generation of the photothermal signal

Light absorption → Light energy into heat conversion → Heat diffusion → Others

Optical properties ↑ Light absorption

e.g. Conversion Efficiency ↑ Light energy into heat conversion

Thermal properties ↑ Heat diffusion

MOTIVATION:

WHY TO USE SUCH EFFECT FOR MATERIALS (e.g. thermal) CHARACTERIZATION

Which thermal properties?

Thermal conductivity [W/mK]

Thermal diffusivity [m^2/s]

$$\alpha = k/\rho c$$

specific heat [J / kg K]

mass density [kg/m^3]

$$C = \rho c$$

Specific (volumen) heat capacity [J / m^3 K]

$$\varepsilon = k/\alpha^{1/2} = (Ck)^{1/2}$$

Thermal effusivity [$Js^{1/2}\ m^{-2}\ K^{-1}$]

Homogenoeus heat diffusion equation

$$\nabla^2 T - \frac{1}{\alpha}\frac{\partial T}{\partial t} = 0$$

Thermal diffusivity becomes the relevant parameter in non-stationary problems

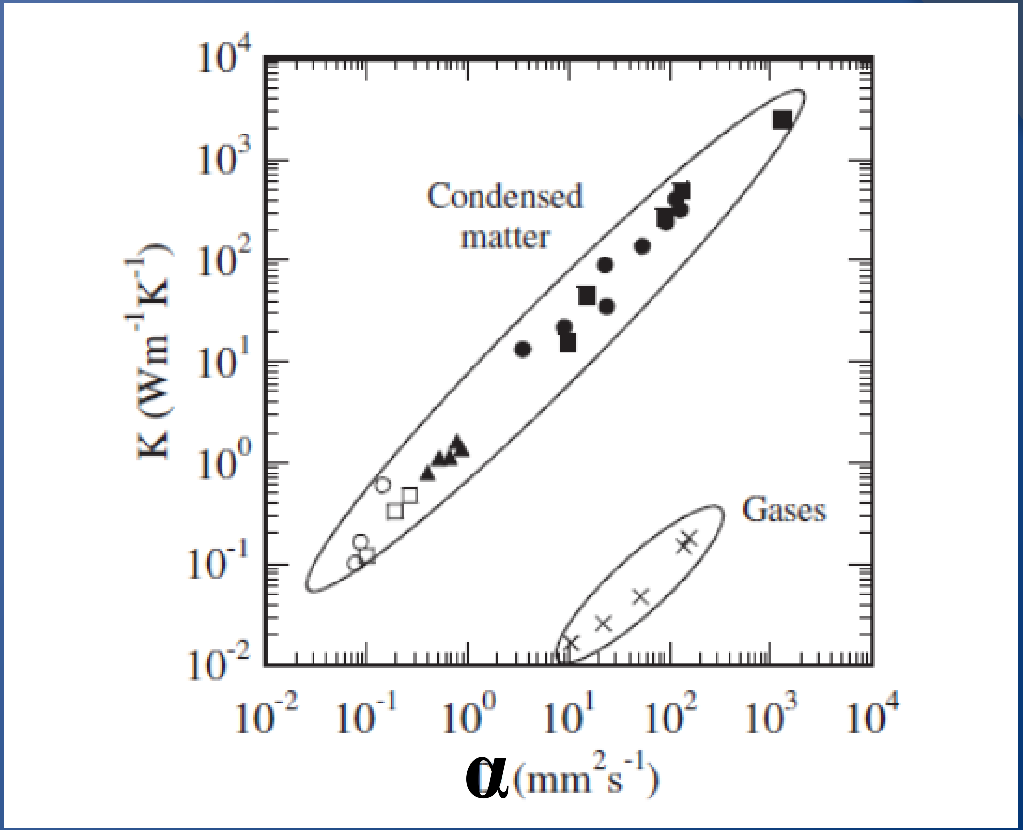

Closed circles: metals; squares: ceramics; triangles: glasses; open squares: polymers; open circles: liquids; crosses: gases

Slope ~ ρC ~ 3×10^6 Jm^{-3} K^{-1}

THERMAL WAVES AND THEIR PROPERTIES

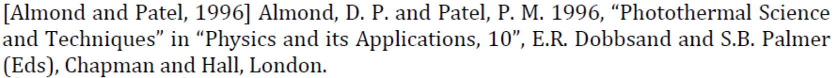
[Almond and Patel, 1996] Almond, D. P. and Patel, P. M. 1996, "Photothermal Science and Techniques" in "Physics and its Applications, 10", E.R. Dobbsand and S.B. Palmer (Eds), Chapman and Hall, London.

Isotropic and homogeneus semi-infinite solid + Superficial uniform light absorption (1D) + $\eta = 1$ + R=0 + neglecting heat losses (with H)


International Journal of Thermal Sciences 98 (2015) 202–207

$$\frac{\partial^2 T(x,t)}{\partial x^2} - \frac{1}{\alpha}\frac{\partial T(x,t)}{\partial t} = 0 \; , \quad x > 0 \, , \; t > 0$$

HDE

$$-k \left.\frac{\partial T(x,t)}{\partial x}\right|_{x=0} = \frac{I_0}{2} Re[(1 + \exp(i\omega t))]$$

BC

$$T(x,t) = \theta(x) exp(i\omega t) \rightarrow \quad \frac{\partial^2 \theta(x,t)}{\partial x^2} - q^2 \theta(x) = 0$$

$$-k \left.\frac{\partial \theta(x,t)}{\partial x}\right|_{x=0} = Re\left[\frac{I_0}{2} exp(i\omega t)\right]$$

$$q = \sqrt{\frac{i\omega}{\alpha}} = \frac{(1+i)}{\mu}$$

Wave number

$$\mu = \sqrt{\frac{2\alpha}{\omega}}$$

Thermal diffusion length

$$T(x,t) = \frac{I_0}{2\varepsilon\sqrt{\omega}} exp(-qx) exp\left[-i\left(\omega t + \frac{\pi}{4}\right)\right] = \frac{I_0}{2\varepsilon\sqrt{\omega}} exp\left(-\frac{x}{\mu}\right) exp\left[-i\left(\frac{x}{\mu} + \omega t + \frac{\pi}{4}\right)\right]$$

THERMAL WAVE EQUATION

Thermal properties determination is possible !

$$\varepsilon = k/\alpha^{1/2} = (Ck)^{1/2} \qquad C = \rho c$$

Thermal effusivity ~ *k* because the almost constancy of *C*

THERMAL WAVES AND THEIR PROPERTIES

$$T(x,t) = \frac{I_0}{2\varepsilon\sqrt{\omega}} exp(-qx) exp\left[-i\left(\omega t + \frac{\pi}{4}\right)\right] = \frac{I_0}{2\varepsilon\sqrt{\omega}} exp\left(-\frac{x}{\mu}\right) exp\left[-i\left(\boxed{\frac{x}{\mu}} + \omega t + \boxed{\frac{\pi}{4}}\right)\right]$$

Amplitude

Phase

$$\Delta\phi = x/\mu + \pi/4$$

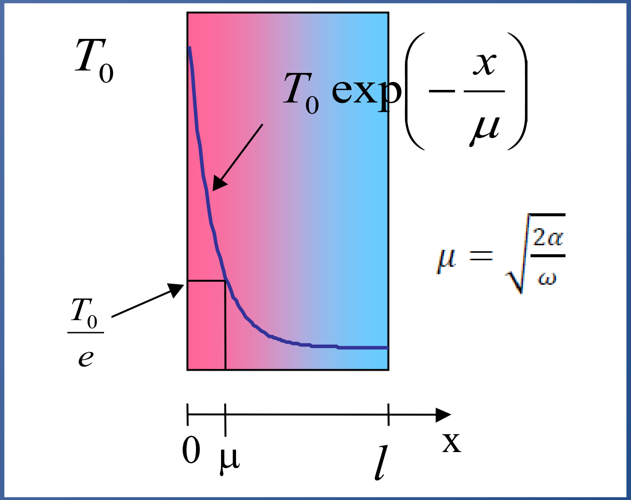

Thermal diffusion length

$$Z_t = \frac{T(x=0,t) - T_{amb}}{-k\frac{dT(x,t)}{dx}\Big|_{x=0}}$$

$$Z_t = \frac{1-i}{\varepsilon\sqrt{\omega}} = \frac{1}{\varepsilon\sqrt{\omega}} exp\left(-i\frac{\pi}{4}\right)$$

Thermal impedance

$$T(x,t) = \frac{I_0}{2} Z_t exp\left(-\frac{x}{\mu}\right) cos\left(\frac{x}{\mu} + \omega t\right)$$

$\lambda = 2\pi\mu$ Wave-length

$$v_f = f\lambda = (\omega/2\pi)(2\pi\mu) = \mu\omega\mu = (2\alpha\omega)^{1/2}$$

$$v_g = 2v_f$$

Phase velocity

Group velocity

THERMAL CHARACTERIZATION BY SLOPE METHOD

$$T(L,t) = \frac{I_0}{2\varepsilon\sqrt{\omega}} exp(-qL) exp\left[-i\left(\omega t + \frac{\pi}{4}\right)\right] = \frac{I_0}{2\varepsilon\sqrt{\omega}} exp\left(-\frac{L}{\mu}\right) exp\left[-i\left(\frac{L}{\mu} + \omega t + \frac{\pi}{4}\right)\right]$$

Amplitude

Phase

$$\mu = \sqrt{\frac{2\alpha}{\omega}}$$

$$\Delta\phi = L/\mu + \pi/4$$

LOG (AMPLITUDE × $\omega^{1/2}$) VERSUS $\omega^{1/2}$

PHASE VERSUS $\omega^{1/2}$

STRAIGH LINE WITH SLOPE = L /$(2\alpha)^{1/2}$

FREQUENCY DEPENDENT INSTRUMENTAL FACTOR
CAN AFFECT BOTH AMPLITUDE AND PHASE
→ NORMALIZATION PROCEDURES, EXPERIMENTAL ARTIFACTS, ETC

LOG (AMPLITUDE) VERSUS L

PHASE VERSUS L

STRAIGH LINE WITH SLOPE = $(\omega/2\alpha)^{1/2}$

STRAIGHFORWARD PROCEDURES

2^{ND} PART:
THE PHOTOTHERMAL BEAM AND MULTIBEAM DEFLECTION TECHNIQUES

MIRAGE EFFECT

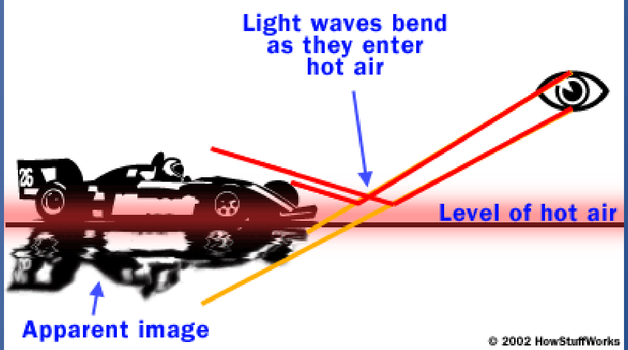

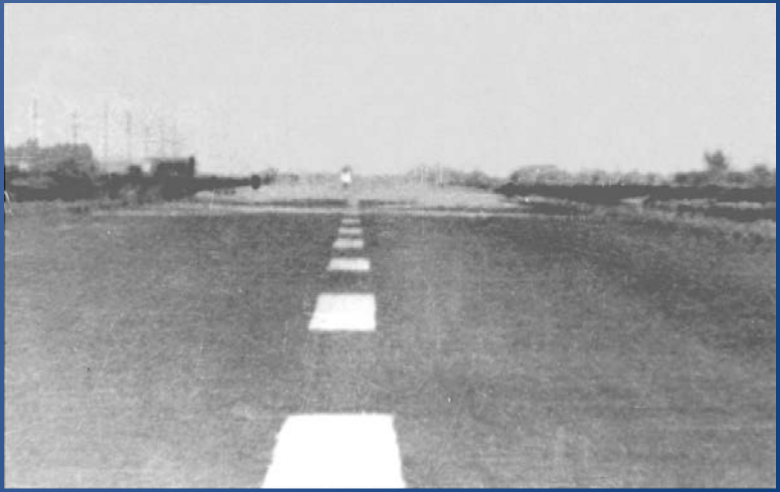

BEAM DEFLECTION TECHNIQUE

$$n \propto \frac{dn}{dT} T_\gamma$$

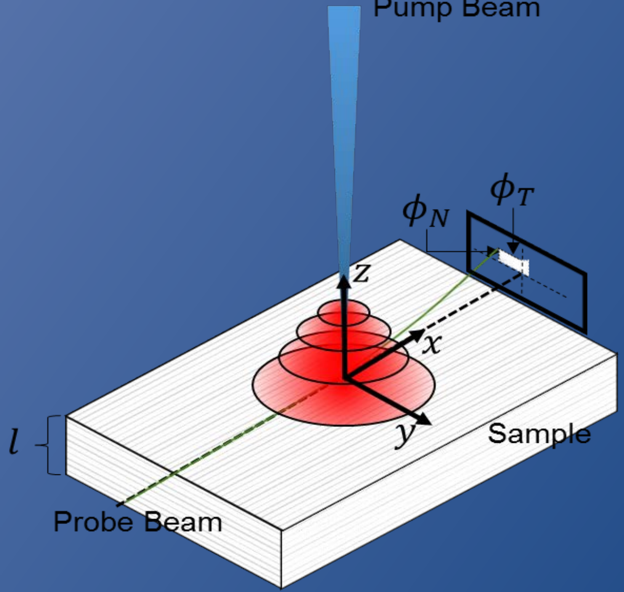

$$\mu_i = \sqrt{\frac{\alpha_i}{\pi f}}$$

$$(\mu_\gamma \ll \mu_s)$$

$$T_\gamma(y) = \frac{P_0}{4\pi k_s}\int_0^\infty \delta J_0(\delta y)\, exp\left(-\frac{(\delta a)^2}{4}\right)\frac{1}{\beta_s} \times \Psi \; d\delta$$

$$\Psi = \frac{1 + exp\left(-2\beta_s l\right)}{1 - exp\left(-2\beta_s l\right)} exp\left(-z\beta_\gamma\right)$$

where P_0 is the exciting beam power, a is the beam radius defined at $1/e^2$ of the beam's intensity, k_s is the sample's thermal conductivity, J_0 denotes the Bessel function of zero order, sub-indexes γ and s represent the medium and the sample respectively and $\beta_i = \delta^2 + \frac{i\omega}{\alpha_i}$ $(i = \gamma, s)$, with δ as the integration variable

$$\phi_T = -\frac{1}{n}\frac{dn}{dT}\frac{P_0}{2\pi K_s} e^{i\omega t}\int_0^\infty \delta \sin(\delta y)\, e^{-\frac{(\delta a)^2}{4}} \beta_s^{-1} \Psi d\delta\, \hat{k}$$

$$\phi_N = -\frac{1}{n}\frac{dn}{dT}\frac{P_0}{2\pi K_s} e^{i\omega t}\int_0^\infty \beta_\gamma \cos(\delta y)\, e^{-\frac{(\delta a)^2}{4}} \beta_s^{-1} \Psi d\delta\, \hat{j}$$

where n is the diffraction index and l is the sample's length in the z direction.

Phase of ϕ_T versus pump to probe offset → straighline with slope m = $(\pi f/\alpha_s)^{1/2}$

A. Salazar, A. Sanchez-Lavega, and J. Fernandez, "Theory of thermal diffusivity determination by the mirage technique in solids," *J. Appl. Phys.*, vol. 65, p. 4150, 1989.

MULTIBEAM DEFLECTION TECHNIQUE

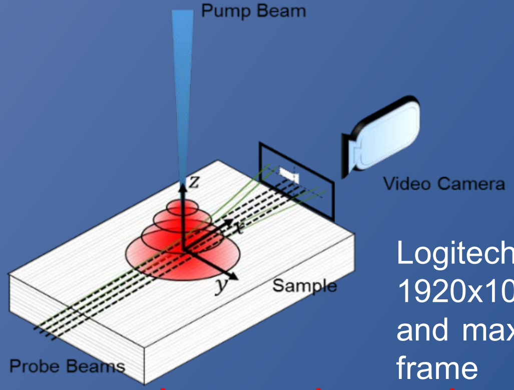

Logitech C920 Webcam
1920x1080 pixels, 8 bit pixel sensitivity and maximum frame rate of 20 fps at full frame

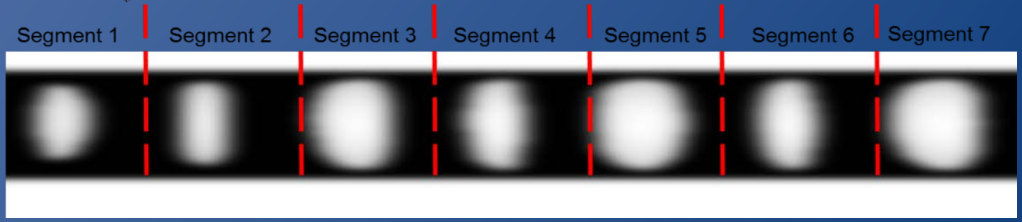

Video is segmenting into as many sections as beams there are

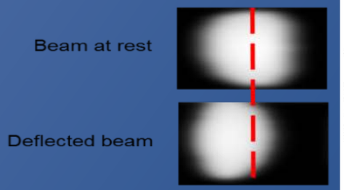

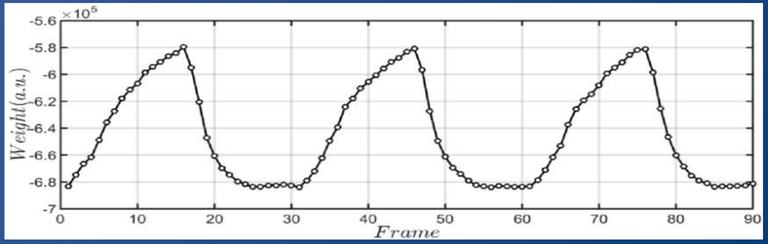

Comparison between the weight of pixels values to the right with those to the left of the vertical section midline (software implementation of a QPD)

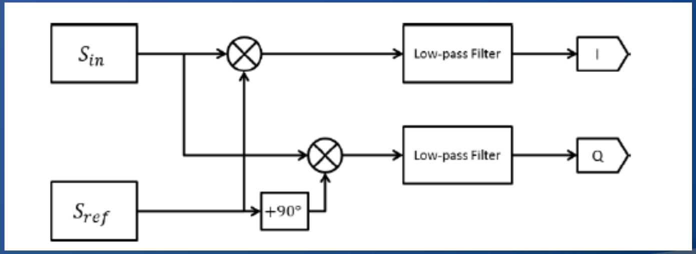

Lock-in amplification

$$\varphi = tan^{-1}\left(\frac{Q}{I}\right)$$

$$A = \frac{1}{2}\sqrt{I^2 + Q^2}$$

LIA in a Nut Shell

$S = A\cos(\omega t + \varphi) + n$
signal to be measured

A: signal amplitude;
φ: signal phase
$\omega = 2\pi f$: angular frequency
n: noise at f

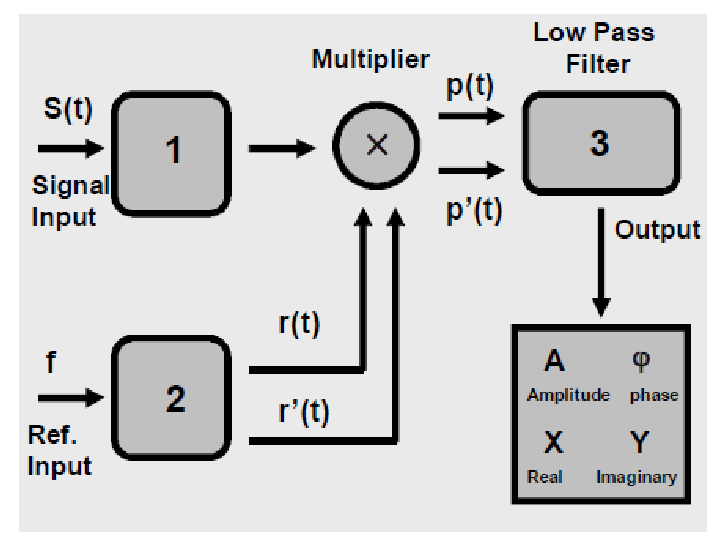

$r = 2\cos(\omega t)$
$r' = 2\sin(\omega t)$

$p = S \times r = A\cos(\varphi) + A\cos(2\omega t + \varphi) + 2n\cos(\omega t)$

$p' = S \times r' = A\sin(\varphi) + A\sin(2\omega t + \varphi) + 2n\sin(\omega t)$

X and Y real (in-phase) and imaginary (quadrature) parts of the complex number A exp $(i\varphi)$; $i = (-1)^{1/2}$

$A = (X^2 + Y^2)^{1/2}$
$\varphi = \mathrm{atan}\,(Y/X)$

$X = A\cos(\varphi)$
$Y = A\sin(\varphi)$

Lat. Am. J. Phys. Educ. Vol.3, No. 3,Sept. 2009

Examples

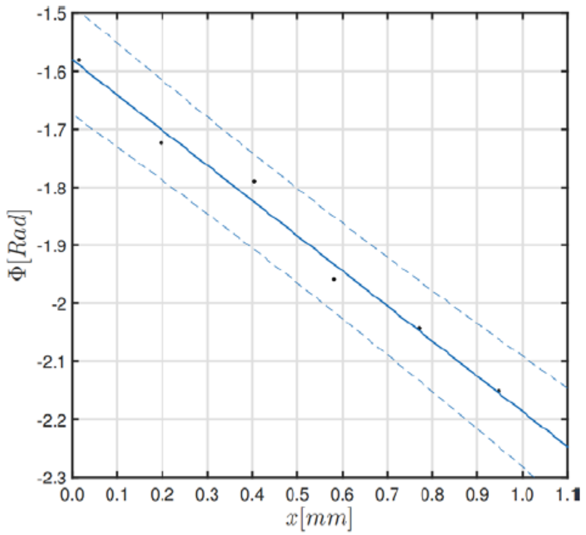

Figure 6 Experimental result for a *CdTe* sample, modulation frequency is 4 Hz. The dots show experimental data, the solid line the best linear fit and the dash lines show the 95% confidence interval for said fit.

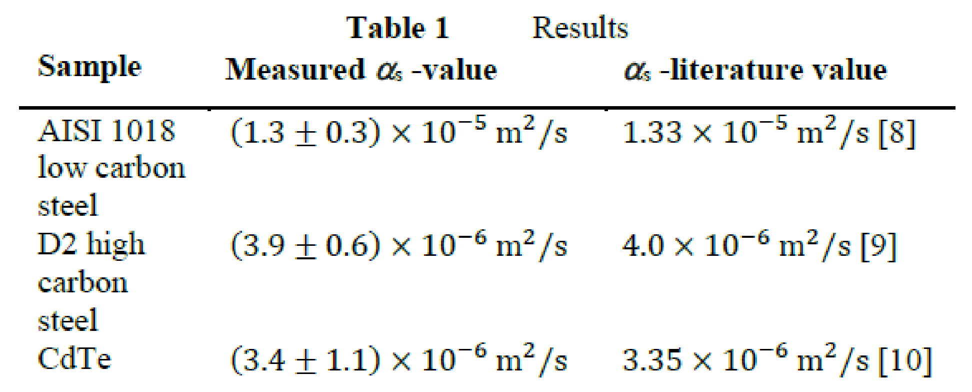

Table 1 Results

Sample	**Measured α_s -value**	**α_s -literature value**
AISI 1018 low carbon steel	$(1.3 \pm 0.3) \times 10^{-5}$ m^2/s	1.33×10^{-5} m^2/s [8]
D2 high carbon steel	$(3.9 \pm 0.6) \times 10^{-6}$ m^2/s	4.0×10^{-6} m^2/s [9]
CdTe	$(3.4 \pm 1.1) \times 10^{-6}$ m^2/s	3.35×10^{-6} m^2/s [10]

3RD PART:
THE PHOTOTHERMAL SHADOWGRAPH METHOD

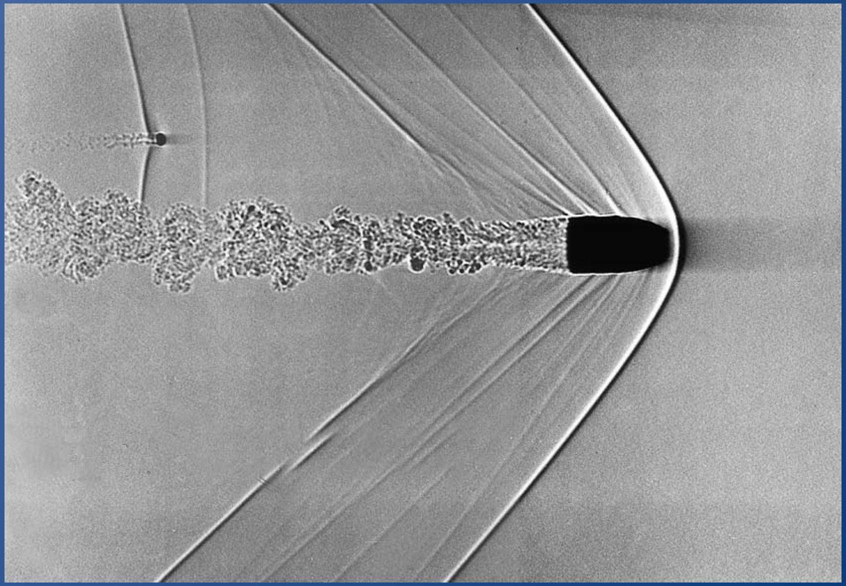

Shadowgraph technique allows to visualize refractive index perturbations in optically transparent of semitransparent media. It is widely used in fluid mechanic, aerodynamik, convection studies, among others

→ Motivation: Can shadowgraph method detect refractive index perturbations in photothermal experiments like beam deflection?

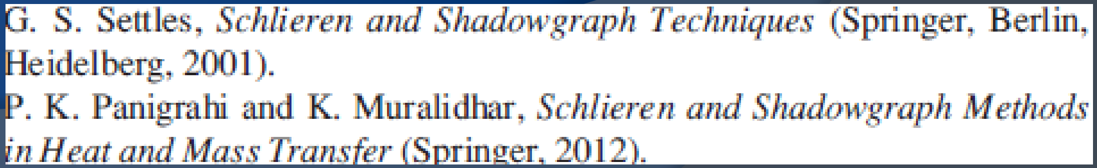

G. S. Settles, *Schlieren and Shadowgraph Techniques* (Springer, Berlin, Heidelberg, 2001).

P. K. Panigrahi and K. Muralidhar, *Schlieren and Shadowgraph Methods in Heat and Mass Transfer* (Springer, 2012).

GOVERNING EQUATIONS

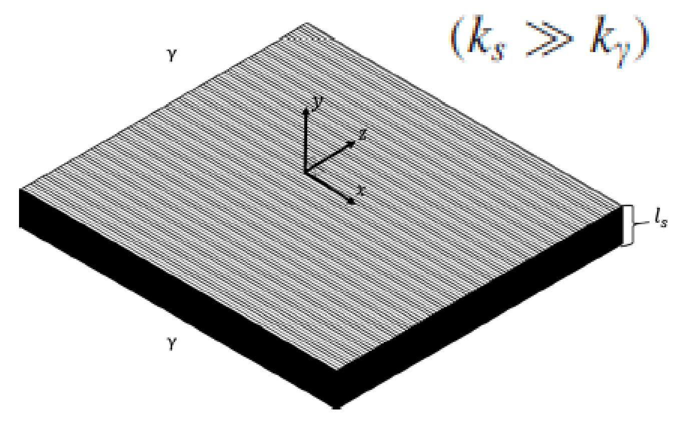

$$T_\gamma(x,y) = \frac{P_0}{4\pi k_s}\int_0^\infty \zeta J_0(\zeta x)\exp\left(-\frac{(\zeta a)^2}{8}\right)\frac{1}{\beta_s} \times \frac{1+\exp(-2\beta_s l_s)}{1-\exp(-2\beta_s l_s)}\exp(-y\beta_\gamma)d\zeta,$$

where P_0 is the excitation beam power, a is the beam radius defined at $1/e^2$ of the beam intensity, k_s is the sample's thermal conductivity, J_0 denotes the Bessel function of zero order, sub-indexes γ and s represent the medium and the sample, respectively, $\beta_i = \zeta^2 + \frac{i\omega}{\alpha_i}$ $(i = \gamma, s)$, and α is the thermal diffusivity. The thermal diffusion length can be defined as $\mu_i = \sqrt{\frac{\alpha_i}{\pi f}}$.

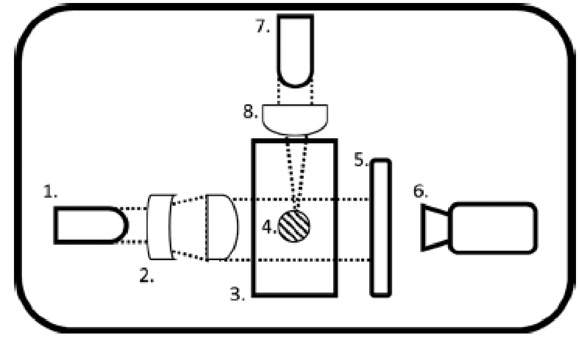

FIG. 4. Experimental configuration. (1) Probe beam, (2) collimating lenses, (3) cell, (4) sample, (5) projection screen, (6) camera, (7) pump beam, (8) focusing lens.

$$n \propto \frac{dn}{dT} T_\gamma$$

$$\frac{I_0 - I_s}{I_s} = (L \times D)\nabla^2 \log(n(x,y))$$

I_0 probe beam intensity; I_s probe beam intensity at projection screen;
L distance between sample and screen; D dimensión parameter; n refractive index

G. S. Settles, *Schlieren and Shadowgraph Techniques* (Springer, Berlin, Heidelberg, 2001).

COMPUTATIONAL SIMULATIONS

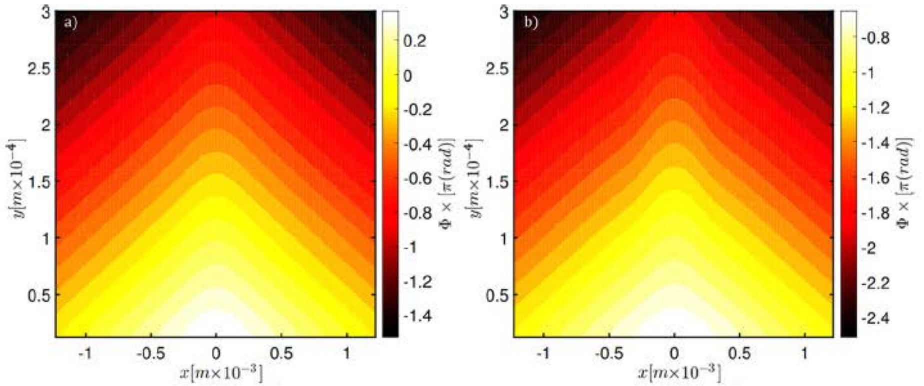

FIG. 2. Simulation results for $\alpha_s = 1.0\times10^{-5}$ $[\mathrm{m^2/s}]$ and 8 Hz modulation frequency. (a) Thermally thin and (b) thermally thick sample.

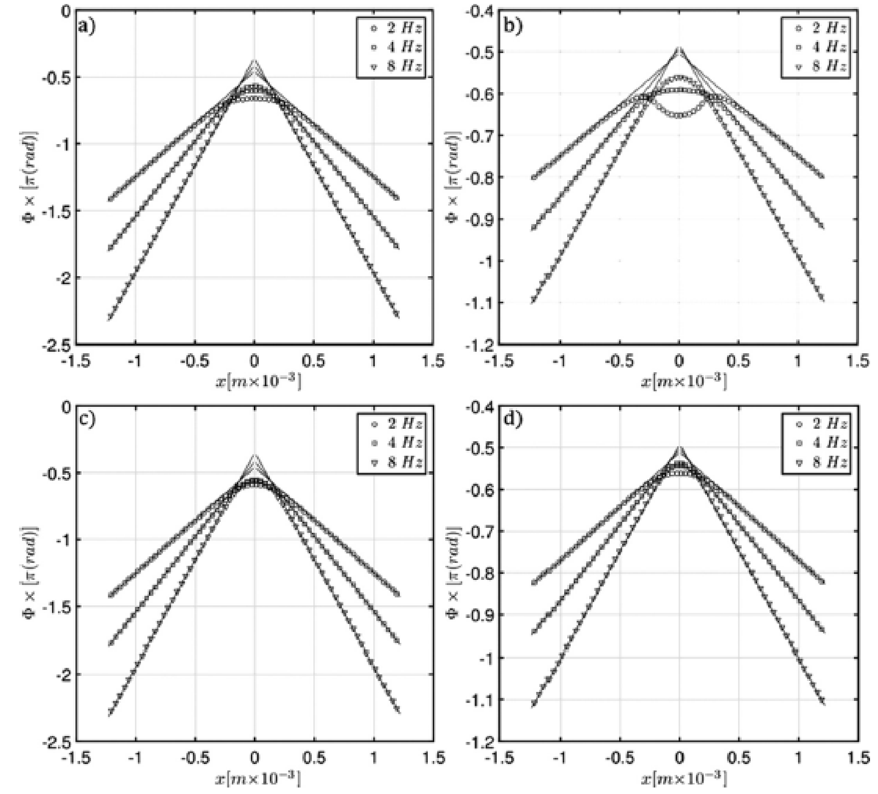

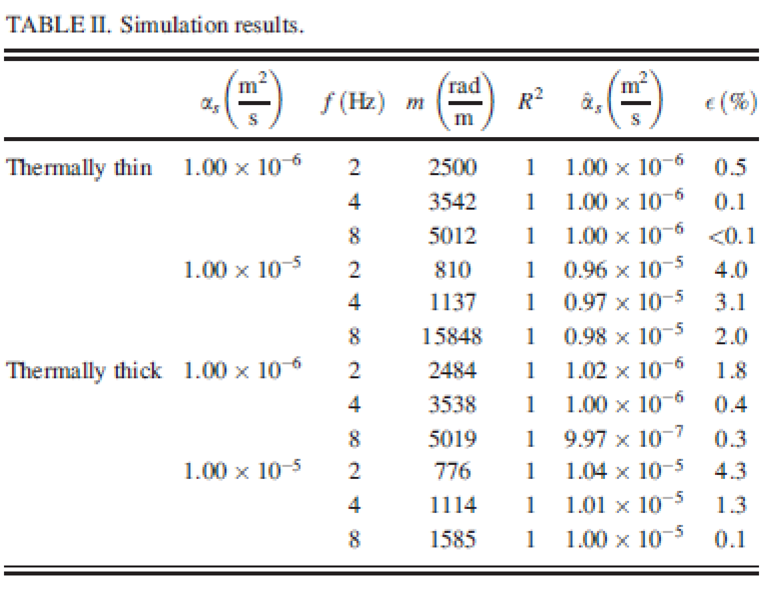

TABLE II. Simulation results.

	$\alpha_s\left(\frac{\mathrm{m}^2}{\mathrm{s}}\right)$	f (Hz)	$m\left(\frac{\mathrm{rad}}{\mathrm{m}}\right)$	R^2	$\hat{\alpha}_s\left(\frac{\mathrm{m}^2}{\mathrm{s}}\right)$	ϵ (%)
Thermally thin	1.00×10^{-6}	2	2500	1	1.00×10^{-6}	0.5
		4	3542	1	1.00×10^{-6}	0.1
		8	5012	1	1.00×10^{-6}	<0.1
	1.00×10^{-5}	2	810	1	0.96×10^{-5}	4.0
		4	1137	1	0.97×10^{-5}	3.1
		8	15848	1	0.98×10^{-5}	2.0
Thermally thick	1.00×10^{-6}	2	2484	1	1.02×10^{-6}	1.8
		4	3538	1	1.00×10^{-6}	0.4
		8	5019	1	9.97×10^{-7}	0.3
	1.00×10^{-5}	2	776	1	1.04×10^{-5}	4.3
		4	1114	1	1.01×10^{-5}	1.3
		8	1585	1	1.00×10^{-5}	0.1

Objective: to estimate termal diffusivity from slope and to obtain the estimation error by comparing it with the actual value used for the simulation

J. Appl. Phys. **119**, 164902 (2016)

JOURNAL OF APPLIED PHYSICS **119**, 164902 (2016)

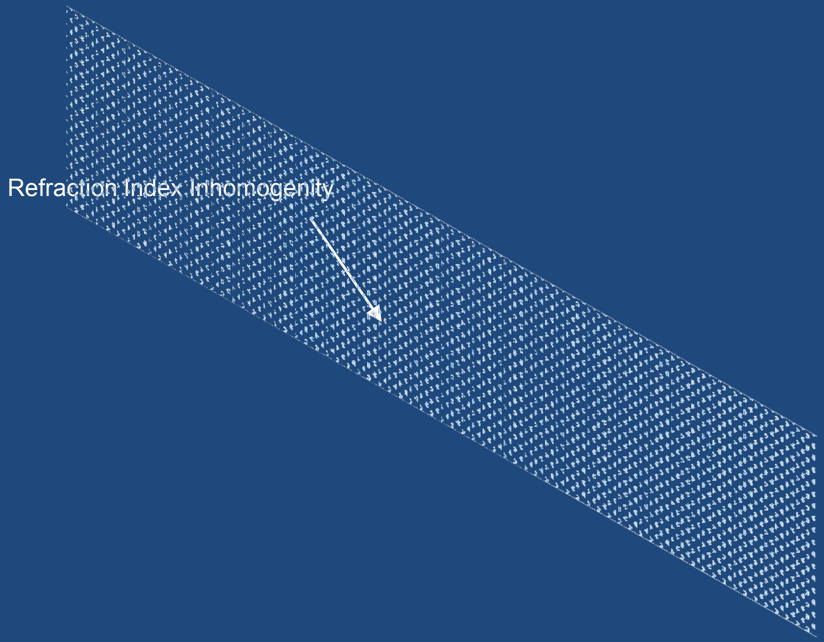

EQUIPMENT

NIR

THERMOGRAPHIC CAMERA FLIR SC2500 NIR
(0.9 – 1.7) μm 320x256 pixel InGaSb, frame rate 340 Hz
(WITH LOCK-IN ON BOARD FACILITIES)

PROBE LASER : 905 nm DIODE LASER

VISIBLE

WEB CAM LOGITECH C920 FULL HS CMOS

PROBE LASER : 630 nm DIODE LASER

PUMP LASER : 445 nm 250 mW (nominal) DL
SAMPLE PLACED WITHIN A 1 cm^3 CELL AND INMERSED IN ACETONITRILE (HIGH dη/Dt)

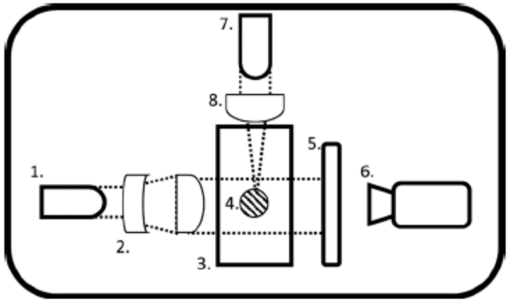

FIG. 4. Experimental configuration. (1) Probe beam, (2) collimating lenses, (3) cell, (4) sample, (5) projection screen, (6) camera, (7) pump beam, (8) focusing lens.

NIR RESULTS

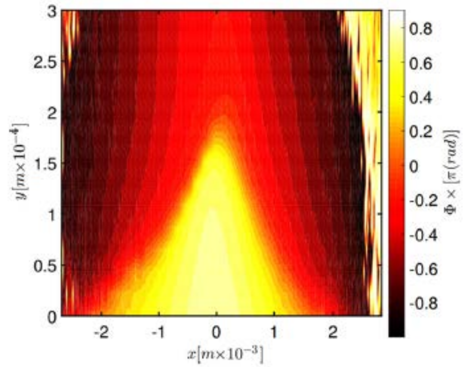

FIG. 5. Phase image resulting from a lock-in shadowgraph of a platinum filament using modulation frequency of 8 Hz obtained with a SC2500 NIR camera.

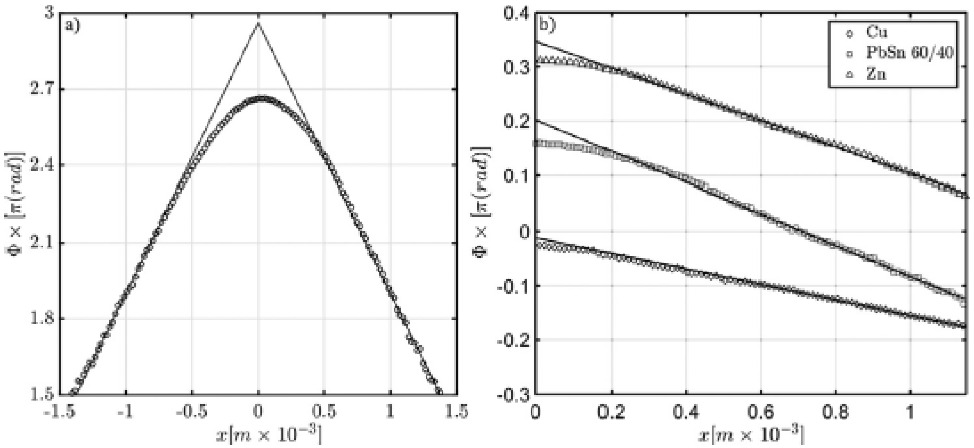

FIG. 6. (a) Phase-lag vs. horizontal offset obtained from the pixel row closest to the platinum filament's surface using modulation frequency of 8 Hz obtained with the SC2500 camera. Solid line shows best least squares linear fit, and bullets show experimental data. (b) Phase lag vs. horizontal offset of the pixel closest to the sample's surface for Cu, PbSn (60/40), and Zn samples.

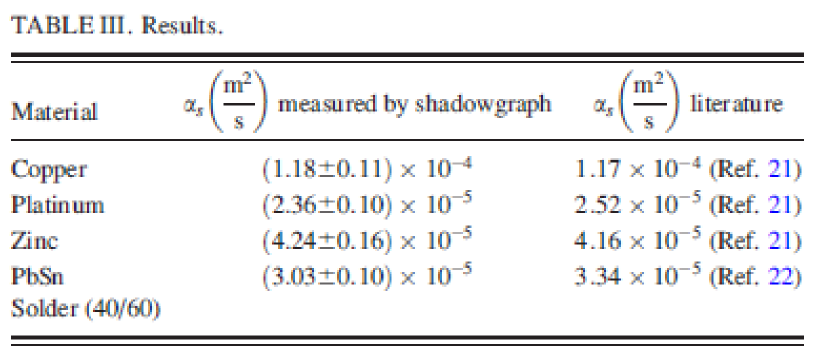

TABLE III. Results.

Material	$\alpha_s\left(\frac{m^2}{s}\right)$ measured by shadowgraph	$\alpha_s\left(\frac{m^2}{s}\right)$ literature
Copper	$(1.18\pm0.11)\times10^{-4}$	1.17×10^{-4} (Ref. 21)
Platinum	$(2.36\pm0.10)\times10^{-5}$	2.52×10^{-5} (Ref. 21)
Zinc	$(4.24\pm0.16)\times10^{-5}$	4.16×10^{-5} (Ref. 21)
PbSn Solder (40/60)	$(3.03\pm0.10)\times10^{-5}$	3.34×10^{-5} (Ref. 22)

J. Appl. Phys. **119**, 164902 (2016)

VISIBLE RESULTS

C920-WEBCAM + DIGITAL LOCK-IN PIXEL BY PIXEL DATA PROCESSING

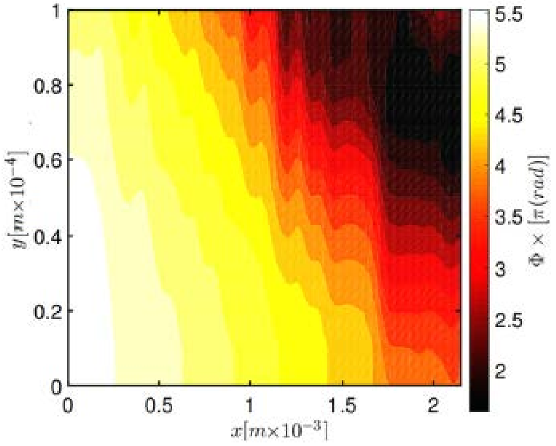

FIG. 7. Phase image of a lock-in shadowgraph of a platinum filament using modulation frequency of 8 Hz obtained with the C920 camera.

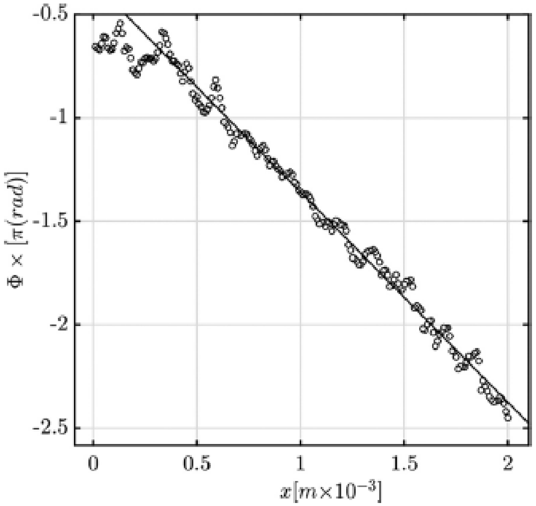

FIG. 8. Phase-lag vs. horizontal offset obtained from the pixel row closest to the platinum filament's surface using modulation frequency of 8 Hz obtained with the C920 camera. Solid line shows best least squares linear fit; symbols show experimental data.

$$\alpha = (2.44 \pm 0.1) \times 10^{-5}\,\mathrm{m}^2/\mathrm{s}$$

J. Appl. Phys. **119**, 164902 (2016)

CONCLUSIONS:

THE PHOTOTHERMAL LOCK-IN SHADOWGRAPH METHOD WAS IMPLEMENTED FOR THE FIRST TIME AND VALIDATED BY THEORETICAL AND EXPERIMENTAL RESULTS.

HIGHLY SPECIALIZED HARDWARE IS NOT REQUIRED FOR THE TECHNIQUE TO WORK; A SIMPLE WEBCAM CAN BE USED AS A SENSING ELEMENT → TECHNIQUE HIGHLY ACCESSIBLE, FOR EXAMPLE FOR TEACHING THERMAL WAVE PHYSICS

ACKNOWLEDGEMENTS

INSTITUTIONS:

IPN

COMISION DE OPERACION Y FOMENTO DE ACTIVIDADES ACADEMICAS DEL I. P. N.
COFAA

CONACYT

CNPq
Conselho Nacional de Desenvolvimento Científico e Tecnológico

NSF

DAAD
Deutscher Akademischer Austausch Dienst
German Academic Exchange Service

ICTP
The Abdus Salam
International Centre for Theoretical Physics

COLLABORATORS:
MANY COLLEAGUES (IN MEXICO AND ABROAD) AND STUDENTS

Thank you!